Anomalous/Lévy Photon Diffusion Theory: Toward a New Parameterization of Shortwave Transport in Cloudy Columns

A. B. Davis
Los Alamos National Laboratory
Space and Remote Sensing Sciences Group
Los Alamos, New Mexico

A. Marshak
National Aeronautics and Space Administration
Goddard Space Flight Center
Climate and Radiation Branch
Greenbelt, Maryland

K. P. Pfeilsticker
University of Heidelberg
Institute for Environmental Physics
Heidelberg, Germany

Introduction

Optically speaking, the earth's cloud-laden atmosphere is a complex scattering/absorbing medium, bounded from below by its spatially variable, often rough, semi-reflective surface. In typical situations, several cloud layers are present, some broken, some not, some dense, some not. The key quantity in solar transport is extinction and it varies spatially from vanishingly small Rayleigh-dominated values in cloud-free areas, hence huge mean-free-paths (MFPs), to many hundreds of km^{-1} in dense cloud or fog, hence photon MFPs (essentially "visibilities") of only a few meters. Figure 1 shows a few photon trajectories that illustrate schematically the huge variance in free path. In such a medium, it is not even clear how to define the MFP, which is after all, just the mean of the free-path distribution.

At visible (VIS) wavelengths, incoming solar photons are eventually reflected back to space or absorbed by the ground, so their trajectories are bounded random walks. However, there are large cloud-to-cloud or cloud-to/from-surface jumps as well as jumps inside the clouds that are enhanced by the internal variability; so the key assumption of many small steps in standard one-dimensional (1-D) diffusion theory is highly questionable. Notwithstanding, this problematic theory is the physical basis of all current 2-stream parameterizations in general circulation models (GCMs). Even in a given layer, domain-average extinction and the associated exponential free-path distribution is not enough to fully characterize photon transport. Rather, we can anticipate photon free-path distributions with much longer tails. In an attempt to reduce the complexity of three-dimensional (3-D) radiative transfer into a 1-D setting, we will therefore postulate "Lévy-stable" or "α-stable" jump distributions, which are

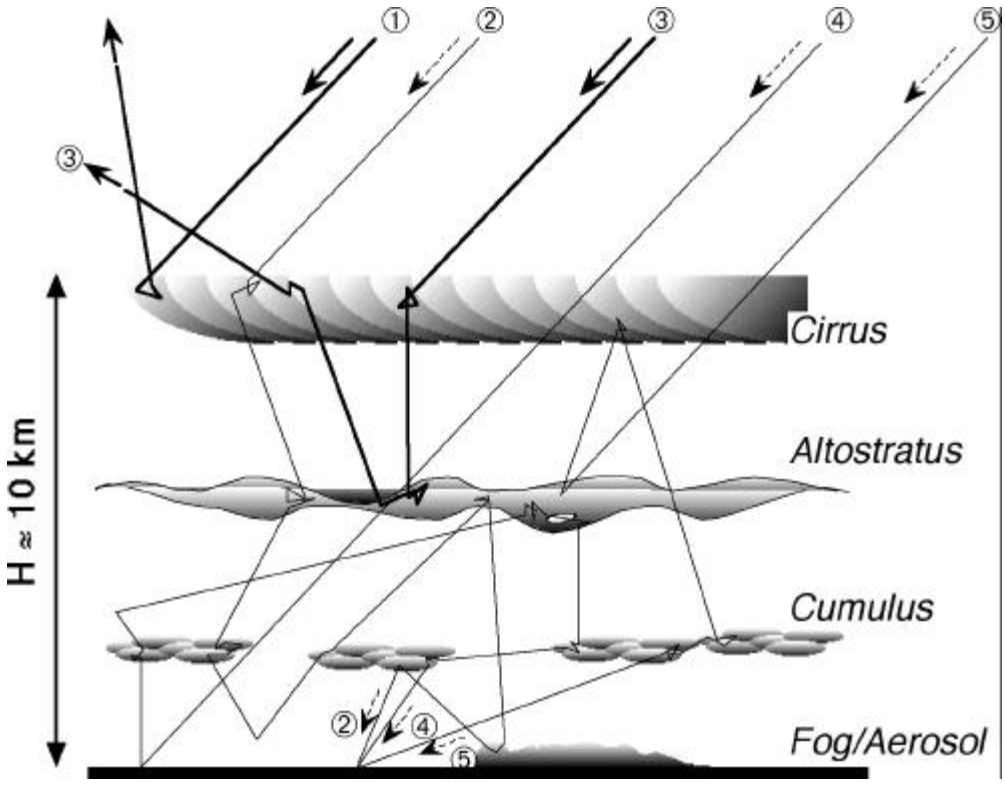

Figure 1. Schematic representation of typical solar photon paths, as observed from the ground. Note the frequent occurrence of long free paths in cloud-cloud and cloud-surface exchanges, as well as the enhanced free paths due to internal cloud variability.

characterized by power-law decays. They depend, beyond the MFP, on a single new parameter, the Lévy index a, which varies between 0 and 2. This puts us into a more general framework to model the photon diffusion (or random-walk) process where "anomalous" laws arise, i.e., photon-to-source distance increases with the $1/\alpha$-power of time, greater than the usual 1/2-power. We retrieve the standard case however in the limit $\alpha \rightarrow 2^{-}$. Because of the sure occurrence of large jumps and the associated faster-that-diffusive transport, random walks with Lévy-distributed steps are often called Lévy-flights." Popularized by Mandelbrot (1982), Lévy-flights have found many applications in statistical physics, chaos theory, fluid dynamics, biology, and finance (e.g., Cambanis et al. 1991; Shlesinger et al. 1995).

The first to focus on Lévy transport in bounded domains, Davis and Marshak (1997) derived asymptotic formulas for transmission probability and mean pathlengths in transmission and reflection that generalize the standard Gaussian case ($\alpha = 2$) to the Lévy case ($\alpha < 2$). By comparison with detailed numerical simulations, these analytic results demonstrate that the Lévy-flight model is a reasonable 1-D approximation to 3-D radiative transfer in an atmospheric column (Davis et al. 1999) with respect to domain-average properties. Pfeilsticker et al. (1998), recently derived solar photon pathlength distributions from ground-based observations of high-resolution oxygen A-band spectra for down-welling zenith radiance under a wide variety of cloud conditions. Pfeilsticker (1999) used these data to empirically determine values of the Lévy index that populate the range $1 \leq \alpha \leq 2$. More

precisely, he finds $\alpha \approx 2$ (steps are Gaussian) under completely overcast skies where a diffusion-domain exists in the sense of King (1987), and he finds $\alpha \approx 1$ when the clouds are very sparse (the MFP actually diverges in this limit, meaning that a single jump is often enough to go from top of [the] atmosphere [TOA] to the ground or vice versa); a large number intermediate cases are also observed. This is essentially, what one expects from first principles and brings strong support to the emerging non-standard 1-D model for bulk solar transport in cloudy skies based on Lévy-flight theory.

In the following sections, we will describe non-technically the properties of Lévy-flights in the logical progression from infinite, to semi-infinite, and to finite domains (including the empirical evidence). Finally, we discuss consequences of the Lévy model for gaseous absorption in the near infrared (NIR) and we report progress towards a new parameterization for shortwave transport in GCMs.

Stable Random Variables

In probability theory, "stability" describes random variables (RVs) that are, in some sense, invariant under addition. This makes them particularly attractive when modeling random walks. Gaussian deviates are the best known example of stability: the sum of n Gaussian RVs is Gaussian with mean and variance obtained by summing those moments for its n components. In general, we ask what independent identically distributed (i.i.d) zero-mean symmetric RVs s_i (i = 1,n) obey

$$\sum_{i=1}^{n} s_i \stackrel{\underline{d}}{=} a_n s_1 \tag{1}$$

where "$\underline{d}$" means equal in distribution. Lévy (1937) showed that the only solutions to this problem have

$$a_n = n^{1/\alpha} \tag{2}$$

with $\alpha \in (0,2]$, and a characteristic function for all s of the form

$$\langle \exp(iks) \rangle = \int \exp(iks) dP(s) = \exp(-\sigma_L |k|^{\alpha}) \tag{3}$$

with $\sigma_L \geq 0$ being a natural amplitude parameter. (Angular brackets $\langle \cdot \rangle$ designate ensemble- or sample-averages throughout the paper.) The well-known Gaussian solution has $\alpha = 2$ and variance $2\sigma_L^2$, so its probability density function (PDF) is

$$dP_2(s)/ds = (1/2\sigma_L \pi^{1/2}) \times \exp[-(s/2\sigma_L)^2]. \tag{4a}$$

Another solution is the Cauchy case with $\alpha = 1$ and PDF given by

$$dP_1(s)/ds = (1/\pi\sigma_L) / [1+(s/\sigma_L)^2]. \tag{4b}$$

These are the only two cases of α-stability with PDFs known in closed form. Interestingly, these two PDFs are the familiar components of the Voigt line profile in spectroscopy: a Doppler core (α = 2), and collisional Lorentzian wings (α = 1).

The main utility of the characteristic function is that its Taylor series expansion at k = 0 yields the moments of s:

$$\langle \exp(iks) \rangle = 1 + \langle s \rangle (ik) + \langle s^2 \rangle (ik)^2 / 2 + \ldots, \tag{5a}$$

as long as all the integrals

$$\langle s^q \rangle = \int s^q dP_\alpha(s), \; q = 0,1,2,\ldots \tag{5b}$$

exist (i.e., are finite). Direct consequences of Eq. (3) are, on the one hand, that $\langle s \rangle$ and other odd-order moments vanish by symmetry and, on the other hand, all the even-order moments exist only if α = 2. If α < 2 then $\langle s^2 \rangle = \infty$. However, a straightforward asymptotic analysis shows that

$$P_\alpha\{s > X\} = \int_X^\infty dP_\alpha(s) \quad \sim X^{-\alpha}; \tag{6}$$

so real-order absolute moments $\langle |s|^q \rangle = \int |s|^q \, dP_\alpha(s) < \infty$ only if q < α. Equation (6) contrasts strongly with the classic result from Beer's law: $P\{s > X\} = a^{-X}$ where a depends on extinction.

In summary, α-stable RVs have infinite variance (q = 2) and even infinite (absolute) means if α ≤ 1. It is important to note that Lévy RVs play the same role as Gaussian RVs with respect to the law of large numbers: PDFs of sums of arbitrary RVs with finite variance tend asymptotically towards Gaussians; PDFs of sums of arbitrary RVs with infinite variance tend asymptotically towards Lévy PDFs.

Finally, there is a simple method for generating symmetric α-stable RVs using uniformly distributed pseudo-RVs ξ ∈ (0,1) that are available in most computer languages or numerical packages. Letting φ = π(1/2–ξ) be uniform on (–π/2,+π/2) and w = –lnξ exponentially distributed with unit mean, then

$$s = \left(\sin\alpha\varphi/(\cos\varphi)^{1/\alpha}\right) \times \left(\cos((1-\alpha)\varphi)/w\right)^{(1-\alpha)/\alpha} \tag{7}$$

is a unitary ($\sigma_L = 1$) symmetric α-stable RV (Samorodnitsky and Taqqu 1994). For α = 2, this reverts to the Box-Muller transform method for generating normal deviates (with variance 2) and, for α = 1, we retrieve the simple formula for unitary Cauchy deviates s = tanφ.

Unbounded Random Walks and Flights

How do we measure particle transport by random walks or flights? The simplest is to define a measure of distance to a source of particles and figure how it evolves with "time," i.e., the number of steps/jumps

or total path covered at some (presumably constant) velocity. To address this question for α-stable step distributions, we return to the sum of i.i.d. symmetric RVs in Eqs. (1) and (2), this time in a 3-D setting:

$$r_n = \sum_{i=1}^{n} s_i \Omega_i \underline{d} = n^{1/\alpha} s_1 \Omega_1, \tag{8}$$

where the Ω_i are unit vectors independently distributed in uniformly random directions.

In the Gaussian case $\alpha = 2$, we can square Eq. (8) and average over all realizations. The crossed terms vanish for lack of correlation between different s_i's and we find

$$\langle r_n^{\,2} \rangle = \sum_{i=1}^{n} s_i^{\,2} = \langle s_1^{\,2} \rangle n. \tag{9}$$

This is just the expression of the additivity of variances of i.i.d. RVs (means of course are also additive, but trivially here because they all vanish). Equivalently, Eq. (9) tells us the root mean square (rms) distance covered by the random walking particle goes as the square root of time. This is the basic law of (standard) diffusion theory.

In the Lévy $\alpha < 2$ case, the above computation is no longer possible because $\langle s_1^{\,2} \rangle = \infty$. However, we still have

$$\langle |z_n| \rangle = \frac{1}{2} \quad \langle |s_1| \rangle n^{1/\alpha}, 1 < \alpha \le 2, \tag{10}$$

and similarly in the other directions ($\langle |\Omega_z| \rangle = 1/2$ for isotropic steps). This reads as an anomalous diffusion law if $\alpha < 2$.

Figure 2 illustrates the dramatic changes in the self-similar geometrical properties of the random walk r_n as α is decreased from 2 to 1.5 and 1.05. The most notable feature of the $\alpha < 2$ cases is the relatively frequent occurrence of jumps with magnitudes at par with $|z_n|$.

Random Walks and Flights in a Semi-Infinite Domain

We are interested in the probability of escape at step n_R of a random walking particle from a semi-infinite domain that it is injected into at step 0 (subscript "R" stands for reflection). It was recently proven by Frisch and Frisch (1995) that this probability is given by:

$$P_{R,\infty}\{n_R > N\} = (2N)!/[2^N (N!)]^2 \sim N^{-1/2}, \text{ as } N \to \infty. \tag{11}$$

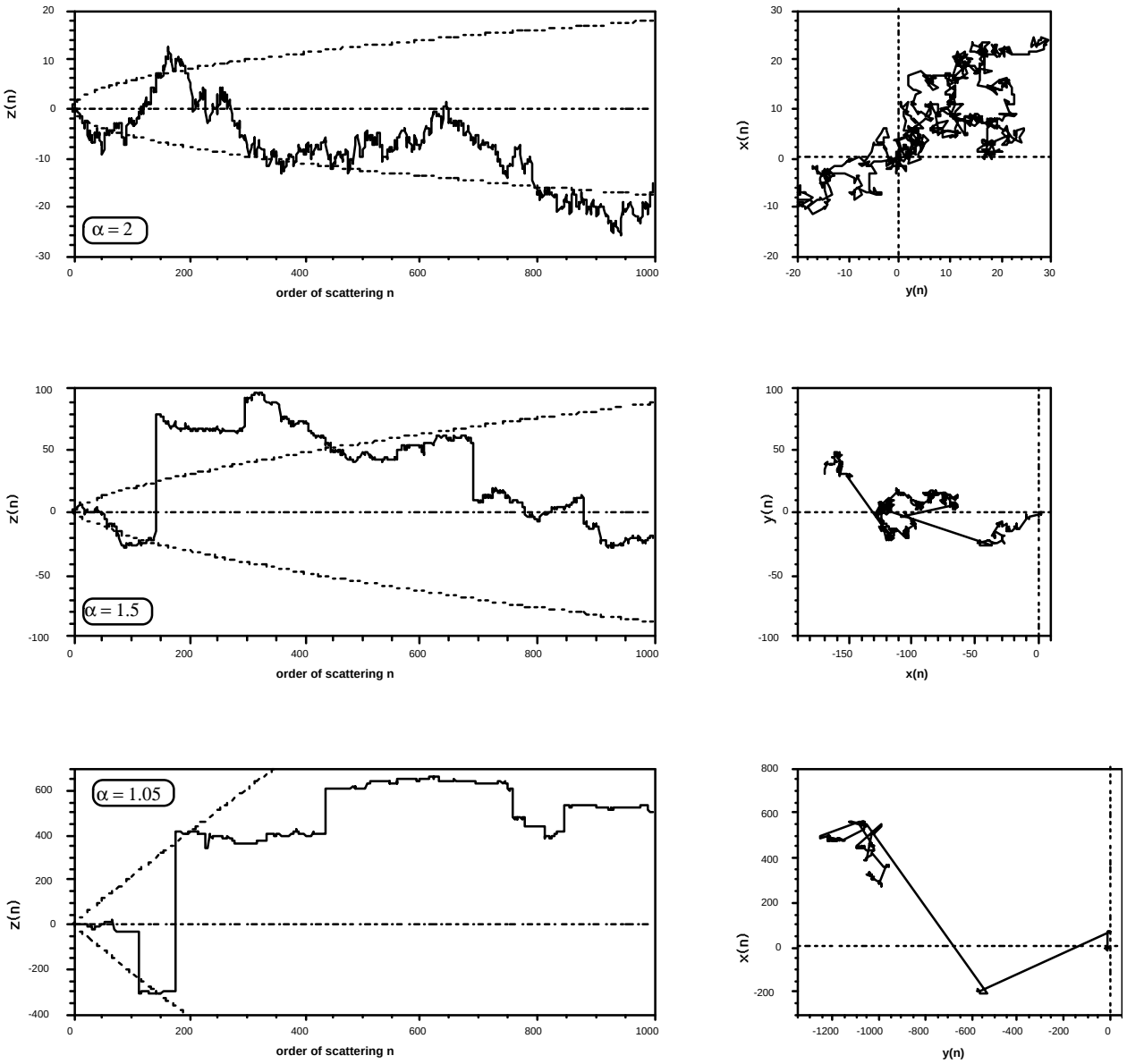

Figure 2. Samples of unbounded random walks ($\alpha = 2$) and flights ($\alpha = 1.5$ and 1.05). 3-D random walks and flights were generated using steps from Eq. (7) in isotropically distributed directions. Notice the rapidly increasing scales from top to bottom. Left-hand side: z(n) with predictions of average position according to Eq. (10). Right-hand side: projection of the 1000-step random walk or flight onto the x,y-plane.

This result does not require that any finite moments exist, only that the steps are symmetrically distributed. Note that, in spite of the fact that $n_R = 1$ with probability 1/2, we have $\langle n_R \rangle = \langle n_R^2 \rangle = \infty$. This is in fact a reminder that, without variance-reduction techniques, Monte Carlo simulations in non-absorbing semi-infinite scattering media will take a long time to execute and/or will lack accuracy. (Incidentally, other numerical schemes such as discrete ordinates also fail in this semi-infinite case.)

Observable Quantities for Bounded Random Walks and Flights

Equations (10) and (11) are the basic ingredients for the asymptotic theory of anomalous diffusion in bounded media, where Lévy-stable (or power-law with divergent variance) step distributions replace the standard exponential or Gaussian ones. All we need is a truncation value in Eq. (11) that depends on the physical thickness H of the medium; this is essentially the average order-or-scattering $\langle n_t \rangle$ for transmitted photons (subscript "T" stands for transmission). For instance, transmission probability is approximated by $T(H) \approx P_{R,\infty}\{n_R \geq \langle n_t \rangle (H)\}$. To obtain $\langle n_T \rangle (H)$ we turn to Eq. (8) and ask, "What is the average of the random n associated with the first occurrence of $r_n \geq H$ (i.e., transmittance)?" Taking a heuristic look at Eq. (10), we set $z_n = H$ and "solve" for this average:

$$\langle n_T \rangle (H) \sim (H/\langle \ell \rangle)^{\alpha} \tag{12}$$

where the notation $\langle \ell \rangle$ is introduced for the MFP $\langle |s| \rangle$. The ratio of the "inner" $\langle \ell \rangle$ and "outer" H scales of the random walk that appears in Eq. (9) can be equated to optical depth τ, at least for $1 < \alpha \leq 2$.

Note that τ and $\langle \ell \rangle$ are the optical depth and MFP for isotropic scattering, also called "transport" optical depth and MFP (Case and Zweifel 1967). Assuming $g \approx 0.85$ (the canonical value for liquid clouds, as obtained from Mie theory), this leads to $1/(1-g) \approx 6.7$ times more than the usual MFP $\langle \ell_{Mie} \rangle$ for forward-peaked scattering and $(1-g) \approx 0.15$ times less than the usual optical depth τ_{Mie}.

In essence, we have generalized here the well-known statement that $\langle n_T \rangle$ goes as τ^2, which is what Eq. (12) yields for $\alpha = 2$. It is important to note here that, because of the boundedness of the domain, all bulk quantities such as the pathlengths discussed below have finite moments of all orders, even though they may be based on local properties such as step distributions that have diverging moments.

Transmission and Albedo

The suggested truncation of the PDF in Eq. (11) using Eq. (12) leads directly to

$$T(H) \sim (H/\langle \ell \rangle)^{-\alpha/2} \sim [(1-g)\tau_{Mie}]^{-\alpha/2}. \tag{13}$$

Equation (10) yields the proper 2-stream limit when $\alpha = 2$, namely (Meador and Weaver 1980): $T(\tau_{Mie}) \sim [(1-g)\tau_{Mie}]^{-1}$. Furthermore, it was checked to high numerical accuracy by Davis and Marshak (1997) for $\alpha < 2$ using the method of generating α-stable steps in Eq. (7).

It is clear that T(H) increases as the variability parameter α in Eq. (10) decreases away from its upper limit 2, the value we can map to homogeneous situations. This was indeed the original motivation of the model, to explain in a 1-D setting the widely known effect of 3-D variability on radiative transfer in cloud layers at non-absorbing wavelengths: albedo $R = 1 - T$ is reduced, transmission T enhanced for a given domain-average optical depth (McKee and Cox 1974; Romanova 1975; Davies 1978; and others).

Figure 3 uses numerical simulations of 1-D trajectories of transmitted Lévy/Gauss particles to illustrate 1) the increase in T(H) with the decrease of α below 2 predicted in Eq. (13), and 2) the decrease in average number of steps for transmitted photons predicted in Eq. (12). In the extreme $\alpha = 2$ case, propagation is very slow and the chance of direct transmission through this slab, about 18 times thicker than the standard deviation of the step, is almost nil. The atmospheric analog is a single well-defined

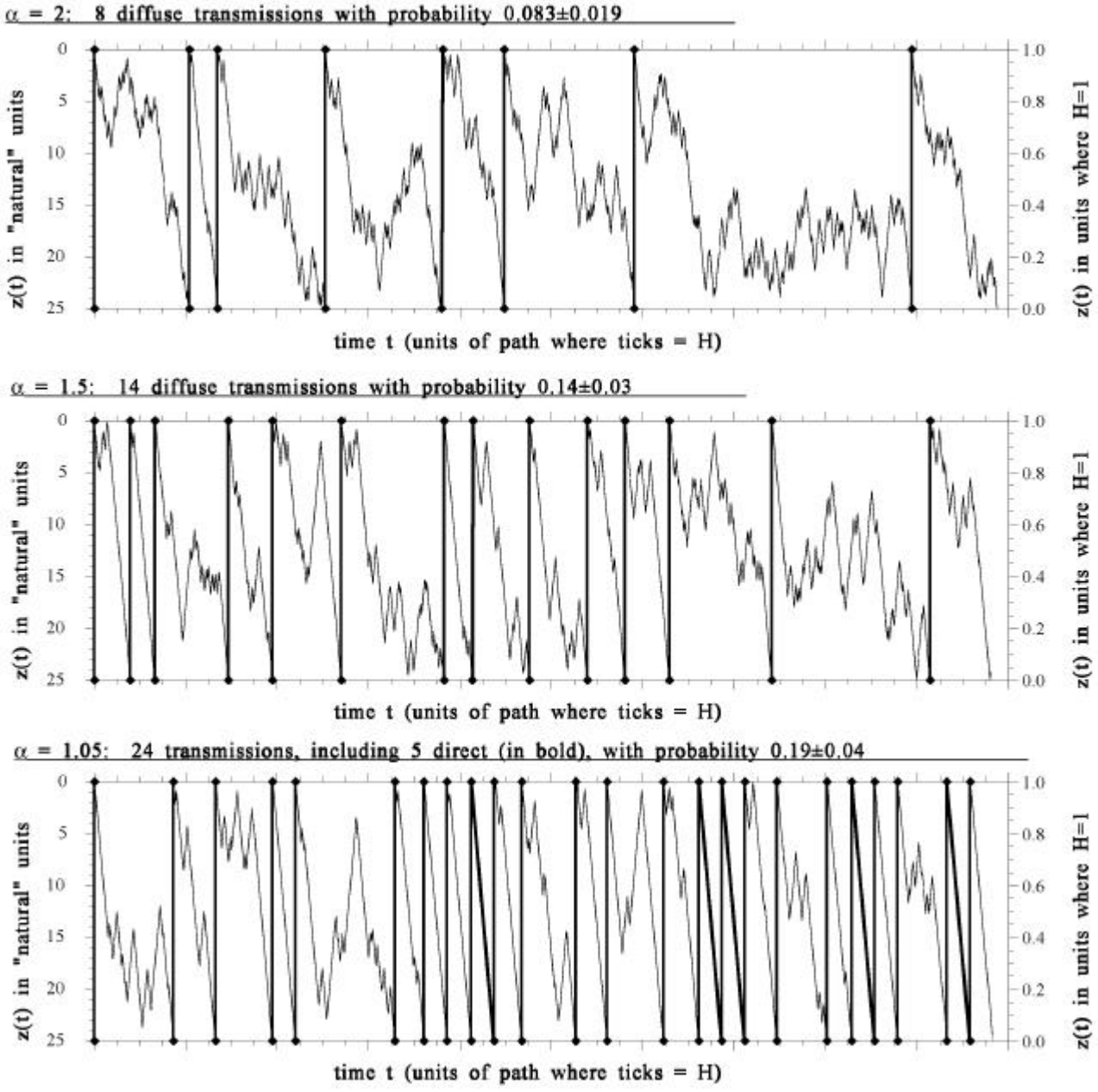

Figure 3. Gaussian walks and Levy Flights through a dense medium. These simulations were selected out of a 100 or so, where all the other trajectories ended in a reflection, some after a very small number of steps, and some after a rather large number of steps when they turn-around just as a transmission almost occurred.

cloud layer, which is optically-thick and only weakly variable, e.g., a stratocumulus deck in the boundary-layer (so the numerical value to assign to H is quite small, 1 km at most). In contrast, the other extreme $\alpha = 1.05$ case exhibits a significant number of direct transmissions that occur without any modification of the multiple-scattering algorithm except the change in α and, otherwise a quite rapid transit through the system is obtained. The atmospheric analog here is a whole cloudy column stretching from the surface to the tropopause (so H is now on the order of 10 km) with several internally variable cloud layers, either optically thin over extended areas or substantially broken, e.g., the situation pictured in Figure 1. This 3-D variability promotes the large jumps that occur naturally in the Lévy model, never within the standard Gaussian framework that supports the diffuse component in all current 2-stream parameterizations. The intermediate $\alpha = 1.5$ case could be mapped to an internally variable single-layer cloud system.

Pathlengths for Transmitted Solar Photons

There is now another observable quantity, which we can use to validate the Lévy-flight model, namely mean pathlength for transmitted solar photons $\langle L_T \rangle$. This is made possible thanks to recent developments in ground-based high-resolution spectrometry applied to the oxygen A-band (Pfeilsticker et al. 1998; Min and Harrison 1999). The specific theoretical prediction for $\langle L_T \rangle$, as given by $\langle \ell_{Mie} \rangle \langle n_{T,Mie} \rangle (H) = \langle \ell \rangle \langle n_T \rangle (H)$ in Eq. (9), is $\langle L_T \rangle (\langle \ell \rangle, H) \sim \langle \ell \rangle^{1-\alpha} H^{\alpha}$, or:

$$\langle L_T \rangle (g, \langle \ell_{Mie} \rangle, H) \sim (1-g)^{\alpha-1} \langle \ell_{Mie} \rangle^{-(\alpha-1)} H^{\alpha}. \qquad (14)$$

Figure 4 shows Pfeilsticker's (1999) data for $\langle L_T \rangle$ and H, both pressure-corrected to account for the strong stratification of the oxygen, overlaid with the predictions in Eq. (11) for $1 \leq \alpha \leq 2$. The agreement is remarkably good given the observational uncertainties. Instrumental details and further discussion are provided by Pfeilsticker et al. (1998) and Pfeilsticker (1999). Note that the g-dependent prefactor in Eq. (14) was not used in this last paper, nor in Figure 3 of Davis et al. (1999); we see here that it makes the range of predictions of the Lévy-flight model more narrow and therefore easier to prove false. This correction notwithstanding, the new model is still compatible with the data, given the error bars assigned a priori to each datum.

Summary, Discussion, and Outlook

We have surveyed the properties Lévy-stable processes unfolding in 3-D infinite and semi-infinite domains, as well as finite 1-D domains. The last case has direct application to the representation of bulk short-wave radiative transfer processes in complex 3-D geometry with a tractable 1-D model. The simple Lévy-flight model for solar photon transport in cloudy atmospheric columns makes specific predictions for quantities readily observable from the ground such as (direct and diffuse) transmission(s) and mean pathlength. The best observations to date support the model.

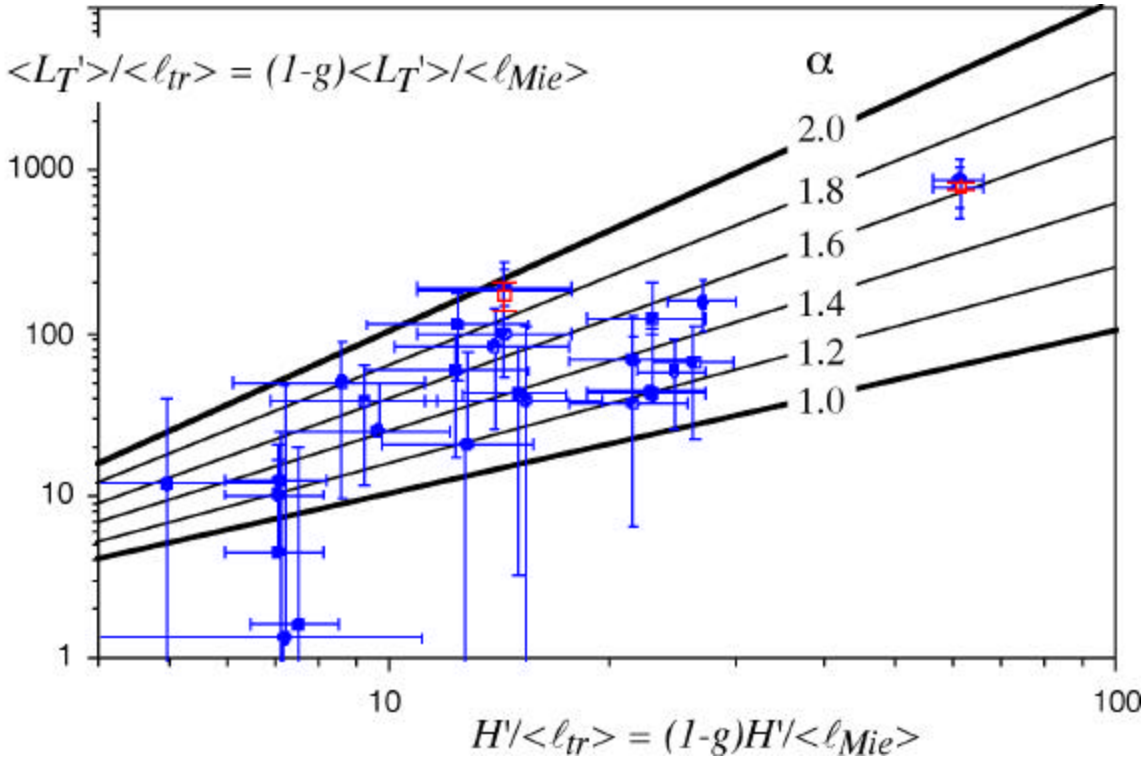

Figure 4. Empirical scatter plot of means pathlength in zenith-radiance versus cloud-layer thickness and Lévy-model predictions. Both lengths are pressure-corrected (hence, the primes in the notations) and non-dimensionalized with MFPs. These were obtained assuming climatology but generous uncertainties were assigned to $\langle \ell_{Mie} \rangle$ and incorporated into the instrumental error bars. The overlaid solid lines are given by Eq. (14), assuming a unit prefactor. As expected from first principles, the observed range of α-values decreases (top to bottom) from 2 to 1 going from completely overcast to almost clear conditions. Note that the impression given here that smaller α leads to smaller pathlengths at a given cloud optical thickness can be off-set and even reversed by the natural variability in H, defined here as the physical thickness of the whole cloud system (see discussion of Figures 1 and 3).

The most stringent test on the model is based on Pfeilsticker's (1999) spectroscopic observations in the oxygen A-band, 768.15 nm to 771.7 nm at 0.0036 nm resolution. Min and Harrison (1999) have recently published some very interesting scatter-plots of τ_{Mie} versus $\langle L_T \rangle$ obtained at Atmospheric Radiation Measurement's (ARM's) Southern Great Plains (SGP) site from A-band measurements at moderate (9 nm) spectral resolution obtained from the Rotating Shadowband Spectroradiometer (RSS). They tend to find longer $\langle L_T \rangle$'s as the cloud situation becomes more complex, for a given τ_{Mie}. This is consistent with the Lévy picture in our Figure 4 because of the different normalization conventions: plotting $\langle L_T \rangle$ in airmasses (essentially one scale-height in our notations) rather than in MFPs. Further analyses are required to ascertain whether the ARM data consolidates or challenges the Lévy-flight model. At any rate, similar findings of longer-than-expected $\langle L_T \rangle$'s using the oxygen B-band and a weak O_2 –O_2 band have also been brought to our attention (Susan Solomon, private communication).

In its status, the Lévy-flight model is well suited for parameterizing short-wave transport in a hypothetical single-layer GCM. Indeed, the model has no way of refining its predictions with information about where the clouds occur in the vertical and what their horizontal properties may be in a given layer. This enhancement would likely call, at a minimum, for an altitude-dependent Lévy index α. This is the variability parameter of the model, leading back to a standard 2-stream prediction in the limit $\alpha \rightarrow 2^{-}$. Also needed is a formulation of the model with differential equations and boundary values. Precisely such formalism, for the moment only for initial-value problems however, has recently been developed by Meerschaert et al. (1999) using fractional-order derivatives.

How does the Lévy-flight model impact gaseous absorption? Pfeilsticker (1999) raises the point that, at the free-path (scatter-to-scatter) level, α-stable step distributions will systematically broaden spectral lines, equivalently, enhance absorption in the continuum. Taking a more global standpoint, we see that as α decreases below 2, $\langle n_T \rangle$ decreases for a given rescaled optical depth ($H/\langle \ell \rangle$) in Eq. (12); however, one can argue that the MFP is inexorably increasing as α decreases, so mean pathlengths $\langle L_T \rangle$, which are more relevant to absorption by well-mixed gases can likely go either way. Anyway, mean pathlengths may not be enough and we may need to look at their whole PDF. Finally, to make inferences about column absorption from pathlength information, we need it at both boundaries, i.e., for transmission and for reflection. Davis and Marshak (1997) derived mean quantities, $\langle n_R \rangle$ and $\langle L_R \rangle$, for the later case but we need airborne A-band data for validation while waiting for the PICASSO/CENA and CloudSat space instruments. In short, the Lévy-flight model's impact on gaseous absorption remains an open question, which is in good keeping with what 3-D cloud variability has had to say about the issue of short-wave column absorption enhancement in presence of clouds: it can go one way or the other (e.g., O'Hirok and Gautier 1998; Marshak et al. 1998).

References

Cambanis, S., G. Samorodnitsky, and M. S. Taqqu, (Eds.), 1991: *Stable Processes and Related Topics*, Birkhäuser, Boston, Massachusetts.

Case, K. M., and P. F. Zweifel, 1967: *Linear Transport Theory*, Addison-Wesley, Reading, Massachusetts.

Davies, R., 1978: The effect of finite geometry on the three-dimensional transfer of solar irradiance in clouds. *J. Atmos. Sci.*, **35**, 1712-1725.

Davis, A., and A. Marshak, 1997: Lévy kinetics in slab geometry: scaling of transmission probability. In *Fractal Frontiers*, Eds., M. M. Novak, and T. G. Dewey, pp. 63-72, World Scientific, Singapore.

Davis, A. B., K. P. Pfeilsticker, and A. Marshak, 1999: The Lévy-flight model for solar photon transport in the cloudy atmosphere: observational support from high-resolution oxygen A-band spectroscopy. In *Proceedings of 10th AMS Conference on Atmospheric Radiation*, pp. 575-578. American Meteorological Society, Boston, Massachusetts.

Frisch, U., and H. Frisch, 1995: Universality in escape from half space of symmetrical random walks. In *Lévy Flights and Related Topics in Physics*, Eds. M. F. Shlesinger, G. M. Zaslavsky, and U. Frisch, pp. 262-268. Springer-Verlag, New York.

King, M. D., 1987: Determination of the scaled optical thickness of clouds from reflected solar radiation measurements. *J. Atmos. Sci.*, **44**, 1734-1751.

Lévy, P., 1937: *Théorie de l'addition des variables aléatoires*, Gauthier Villars, Paris.

Mandelbrot, B. B., 1982: *The Fractal Geometry of Nature*, W. H. Freeman, San Francisco, California.

Marshak, A., A. Davis, W. J. Wiscombe, W. Ridgway, and R. F. Cahalan, 1998: Biases in shortwave column absorption in the presence of fractal clouds. *J. Climate*, **11**, 431-446.

McKee, T. B., and S. K. Cox, 1974: Scattering of visible radiation by finite clouds. *J. Atmos. Sci.*, **31**, 1885-1892.

Meador, W. E., and W. R. Weaver, 1980: Two-stream approximations to radiative transfer in planetary atmospheres: A unified description of existing methods and a new improvement. *J. Atmos. Sci.*, **37**, 630-643.

Meerschaert, M. M., D. A. Benson, and B. Bäumer, 1999: Multidimensional advection and fractional dispersion. *Phys. Rev. E*, **59**, 5026-5028.

Min, Q., and L. Harrison, 1999: Joint statistics of photon pathlength and cloud optical depth. *Geophys. Res. Lett*. In press.

O'Hirok, W., and C. Gautier, 1998: A three-dimensional radiative transfer model to investigate the solar radiation within a cloudy atmosphere, Part I: Spatial Effects, *J. Atmos. Sci.*, **55**, 2162–2179, Part II: Spectral Effects, *J. Atmos. Sci.*, **55**, 3065-3076.

Pfeilsticker, K., 1999: First geometrical pathlength distribution measurements of skylight using the oxygen A-band absorption technique – II. Derivation of the Lévy-index for skylight transmitted by mid-latitude clouds. *J. Geophys. Res.*, **104**, 4101-4116.

Pfeilsticker, K., F. Erle, O. Funk, H. Veitel, and U. Platt, 1998: First geometrical pathlength distribution measurements of skylight using the oxygen A-band absorption technique – I. Measurement technique, atmospheric observations, and model calculations. *J. Geophys. Res.*, **103**, 11,483-11,504.

Romanova, L. M., 1975: Radiative transfer in a horizontally inhomogeneous scattering medium. *Izv. Acad. Sci. USSR Atmos. Oceanic Phys.*, **11**, 509-513.

Samorodnitsky, G., and M. S. Taqqu, 1994: *Stable Non-Gaussian Random Processes*, Chapman and Hall, New York.

Shlesinger, M. F., G. M. Zaslavsky, and U. Frisch (Eds.), 1995: *Lévy Flights and Related Topics in Physics,* Springer-Verlag, New York.